

Numerical simulation of turbulent flow in channels with three-dimensional blocks

Mehdi Ahmadi^{1,*}, Iman Soleimani Marghmaleki²

1. Islamic Azad University, Shahrekord Branch, Ardal Center, Iran
2. Shahrekord University, Shahrekord, Iran

M_Ahmadi@iaushk.ac.ir

Abstract: Turbulent flow over surfaces roughened by simple geometric elements, such as discrete three-dimensional protuberances, continue to be of interest in fluid engineering from several perspectives, regular roughness elements are routinely used for heat transfer enhancement. They are also used to study surface roughness effects, in general, as they easily reproduced in the laboratory and modeled in numerical experiments. The characteristics of a turbulent flow in channels with three-dimensional blocks are investigated in the context of surface roughness effects. Reynolds-averaged, Navier-Stokes equations, coupled with the κ - ω turbulence model with near wall treatment are solved by a finite-volume method. The space-averaged velocity profile exhibits a logarithmic region, with a roughness function that varies logarithmically with the roughness Reynolds numbers. At sufficiently large distance from the roughness elements, the effect of the individual elements vanishes and the net effect on the velocity profile is felt as reduction in the constant, β , known as the roughness function, depends not only on the roughness size but also on its geometry. The different block arrangements exhibit quite distinct flow characteristics but the differences tend to vanish as the block height decreases. In general, Reynolds-averaged numerical model successfully describes the principal features of wall roughness that have hitherto for been the purr view of experimental correlations. [Mehdi Ahmadi, Iman Soleimani Marghmaleki. **Numerical simulation of turbulent flow in channels with three-dimensional blocks**. Life Science Journal. 2011;8(4):511-516] (ISSN:1097-8135). <http://www.lifesciencesite.com>.

Key words: Distributed roughness, Similarity law, RANS equation, κ - ω model

1. Introduction

Turbulent flow over surfaces roughened by simple geometric elements, such as three-dimensional protuberances, continues to be of interest in fluids engineering from several perspectives [1]. Regular roughness elements are routinely used for heat transfer enhancement [2], [3]. They are also easily reproduced in the laboratory and modeled in numerical experiments. Of particular concern in practical engineering applications is the existence of similarity laws, principal among which is the logarithmic velocity distribution, upon which friction factor and heat transfer correlations are based.

At sufficiently large distance from the roughness elements, the effect of the individual elements vanishes and the net effect on the velocity profile is felt as reduction in the constant, β , in the logarithmic law. This change in the constant, β , known as the roughness function, depends not only on the roughness size but also on its geometry [1], [4].

The importance of similarity laws in engineering correlations of friction and heat transfer mentioned above, and the success of these recent numerical studies suggest that a more comprehensive numerical investigation would yield useful insights into the effects of discrete roughness elements on these parameters. As neither LES nor DNS are cost effective for such

purposes, here we use a numerical model based on the Reynolds-Averaged Navier-Stokes (RANS) equations and an established two-equation turbulence model to study the effect of different types of discrete roughness on the velocity profile and related correlations. In particular, the existence of a logarithmic layer is examined and the relevant parameters are identified. Although the RANS approach is not suitable for capturing the flow unsteadiness due to large-eddy motions, it is quite adequate for the present study in which only the mean quantities, both in time and space, are of interest. Calculations are carried out for three-dimensional roughness elements. A brief description of the numerical model is presented as the various components are quite well established, and a simple validation study is performed before describing the principal results.

2. Numerical model and validation

2.1 Governing equations

For steady incompressible turbulent flow, the Reynolds averaged equations for conservation of mass and momentum may be written as follows:

$$\text{Continuity: } \frac{\partial u_i}{\partial x_i} = 0 \quad (1)$$

Momentum:

$$\frac{\partial}{\partial x} [\mathbf{uu} - (v + v_t) \frac{\partial u}{\partial x}] = -\frac{1}{\rho} \frac{\partial P}{\partial x} + \frac{\partial}{\partial x} [v_t \frac{\partial u}{\partial x}] \quad (2)$$

where u is the velocity component x -direction, P is pressure, v is kinematic viscosity and v_t is the eddy viscosity obtained from the turbulence model.

Among several variations of widely used two-equation turbulence models, the low Reynolds-number (near-wall) properly resolve the complex flow behind around the ribs, following the work of [6]. This particular model is chosen because of its proven robustness and unambiguous near-wall treatment, two essential attributes in numerical modeling of separated flow about distributed ribs. The eddy viscosity is determined from two transport equations:

Turbulence kinetic energy (k):

$$(3) \frac{\partial}{\partial x} [\mathbf{uk} - (v + \frac{v_t}{2}) \frac{\partial k}{\partial x}] = P_k - \beta^* k \omega$$

$$R_{P_k} = \frac{k}{\omega \nu} \cdot \beta^* = \frac{9}{100} \cdot \frac{4/15 + (Re_\nu/Re_\tau)^2}{1 + Re_\nu/Re_\tau}, \quad R_\beta = \beta \quad (4)$$

Specific dissipation rate (ω):

$$(5) \frac{\partial}{\partial x} [\mathbf{u\omega} - (v + \frac{v_t}{2}) \frac{\partial \omega}{\partial x}] - \alpha \frac{\omega}{k} P_k - \beta \omega^2$$

$$\alpha^* = \frac{3/125 + Re_\nu/Re_\tau}{1 + Re_\nu/Re_\tau}, \quad R_k = 6$$

$$\alpha = \frac{13}{25} \frac{1/9 + Re_\nu/Re_\tau}{1 + Re_\nu/Re_\tau} \frac{1}{\alpha^*}, \quad R_\omega = 2.95, \quad \beta = \frac{9}{125}$$

$$P_k = v_t \left(\frac{\partial u_i}{\partial x_j} + \frac{\partial u_j}{\partial x_i} \right) \frac{\partial u_i}{\partial x_j}$$

Where P_k the production of turbulence kinetic energy and the eddy viscosity is related to k and ω as:

(6) **2.2. Computational domain and boundary conditions**

The no-slip condition is applied on walls of the channel (Figs. 1 and 2).for developed flow in a long channel with regularly spaced roughness elements; the flow is periodic in the stream wise direction. Then it suffices to consider a limited solution domain and impose periodic conditions at the upstream and downstream boundaries. For a channel with three-dimensional roughness, plane-of-symmetry conditions are applied at appropriately located span wise boundaries. The specific dissipation rate, ω is specified at the first grid off the solid surface and given a value $\frac{6\nu}{(9\Delta n^2/125)}$ where Δn denotes the normal distance from the wall [6].more details on channel geometry, grid and flow conditions are given in later sections.

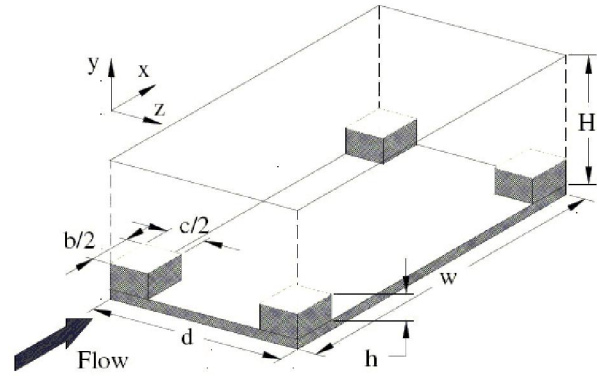


Figure.1. Schematic of channel with distributed hexahedral blocks (staggered distribution), ($h = 0.1, b = 0.3, H = 0.5, d = 0.75$ are fixed).

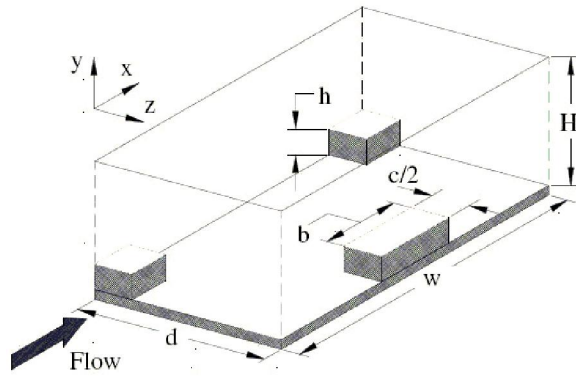


Figure.2. Schematic of channel with distributed hexahedral blocks (in-line distribution), ($h = 0.1, b = 0.3, H = 0.5, d = 0.75$ are fixed).

2.3 Numerical solution procedure

The above equations are solved by a finite-volume method in an orthogonal body-fitted grid.

Second-order accuracy is assured by adopting the central differencing scheme throughout except for the convective derivatives that are discretized by the QUICK scheme of [7]. The continuity and the momentum equations, and the model equations for k and ω , are solved iteratively until convergence. The convergence criterion imposed in the calculation is that the sum of the residuals of mass source be less than 10^{-10} .

2.4. Validation tests

The major difficulty of model validation in the present case is the lack of adequately detailed experimental data for various rib shapes and block arrangements. In view of this, model validation is focused on two important features of the analysis: computation of separated flow and implementation of an orthogonal grid system.

The numerical model outlined above is validated against two test cases, namely, the backward facing step flow, and the square-ribbed channel flow, for which

previous calculations provide a basis for comparison. Other researchers have also used these cases to validate their solution procedures and turbulence models. Therefore, it suffices to provide a very brief description of the results.

Fig.3. Backward facing step flow for $Re_h = 2800$ and $\delta_b/h = 1.1$ at $x/h = -3.8$: (a) streamlines and pressure contours; (b) c_f distribution along the channel. For the backward facing step flow, calculations were performed in a solution domain $-3.8 < x/h < 80$ with a grid $180 \times 80 \times 240$, in which 30 of the 80 grid points are distributed in the expanded region, for a Reynolds number (Re_h), based on step height h and the mean inlet velocity, of 2800. The inlet velocity profile is constructed to match the turbulent boundary layer of the experiment, i.e. $\delta/h = 1.1$. Fig. 3 shows the overall flow field and the friction coefficient along the wall downstream of the step. There is good agreement with the measurements of [8]. The computed reattachment length of $6.67h$. These results provide a degree of validation of the numerical method and turbulence model.

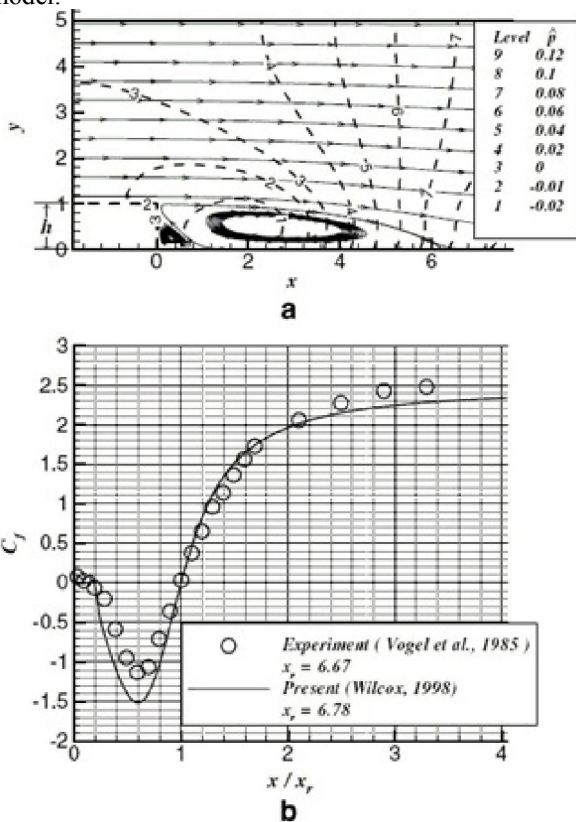


Figure.3. Backward facing step flow for $Re_h=2800$, (a) streamlines and pressure contours, (b) C_f distribution along the channel.

Finally, the flow over the regularly distributed square ribs with $h/D_e = 0.1$ and $w/h = 7.2$ where D_e is the hydraulic diameter, is examined for

$Re_{D_e} = 7,200$. The mean velocity profiles at various cross-sections plotted in Fig.4 are seen to be in good agreement with the measured data of [9].

The discrepancy observed near the top surface of the rib, where the mean velocity attains a local maximum, was first suspected to be due to the insufficient grid resolution ($100 \times 80 \times 256$). An additional calculation with much finer grid ($160 \times 150 \times 256$) confirms that the solution is indeed grid-independent. The two-layer model of [10] may be the only exception that qualitatively shows the local maximum in the mean velocity in that region. The results of the standard $k-\omega$ model with the wall function are shown in the figure for reference.

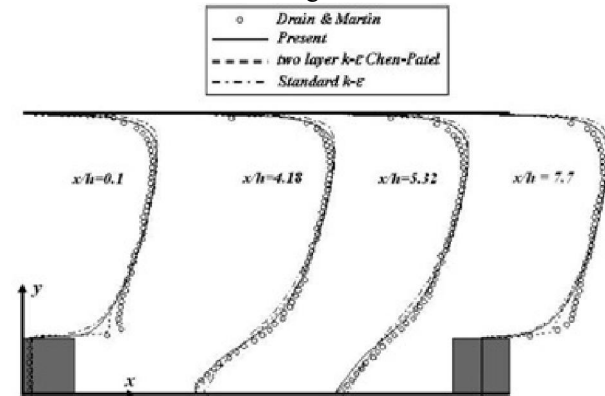


Figure.4. the mean velocity profiles at various cross-sections.

3. Results and discussion

For rough surfaces, the logarithmic velocity profile in the wall region differs from that on a smooth surface, and takes following form:

$$(7) u^+ = \frac{1}{k} \ln(y^+) + B - \Delta B$$

Where $k (= 0.418)$ is the Von Karman constant, B is the smooth-wall constant ($= 5.45$), and ΔB the roughness function, which increases with roughness size. The distance y^+ is measured from the so-called virtual origin y_0 of the wall, which also increases with increasing roughness. May be rewritten as:

$$(8) u^+ = \frac{1}{k} \ln(y^+) + R^+$$

Where:

$$(9) R^+ = \frac{1}{k} \ln(h^+) + B - \Delta B$$

Where:

$$h^+ = \frac{h u_{\tau}}{\nu} \tag{10}$$

For sufficiently large roughness, in the so-called fully rough regime, R^+ is constant and assumes the value of 8.5 for sand-grain roughness [11].

The numerical simulations of three-dimensional flow over uniformly distributed hexahedral blocks, compared to the two-dimensional cases, there are many more geometric parameters to deal with. For present purposes, however, we examine two representative block

cross-sections: a square section and a rectangular section of spanwise aspect ratio of in-line and staggered arrangements, as shown in Fig. 1 and Fig.2. The transverse block spacing d/D_s and streamwise length of the block b/D_s are held constant at 0.75 and 0.3, respectively. The block height and pitch (streamwise spacing) are parameters that are varied. For $w/h = 15$ and 18, a non-uniformly distributed grid of $512 \times 240 \times 240$ cells is used while a grid with $250 \times 150 \times 150$ cells is used for $w/h = 6, 9$ and 12.

Typical flow patterns (not shown) exhibit that the flow around the staggered block is much more violent than that around the in-line blocks, in which the disturbance appears to be confined to immediate neighborhood of the block. The fluid passes between the distributed blocks in fairly orderly fashion for the in-line arrangement, while that for the staggered arrangement meanders around the obstacles and makes the vertical motion very intense. This is clearly illustrated in the cross-flow pattern of each case in Fig. 5. Fig. 5(a) shows the cross-plane streamlines at $x/D_s = 0.6$ for the staggered rectangular blocks. Two large and strong vortices span the entire channel. For the other three cases, on the other hand, the vertical motion is not as intense and is confined to the vicinity of the wall. This is true even for the rectangular block if the distribution is in-line and the square blocks in the staggered arrangement.

As is in two-dimensional case, the skin friction and pressure distributions are integrated over appropriate surface areas to calculate the effective total resistance:

$$(11) \tau_x = \frac{1}{wd} \left[\int_{s_x} (P_w - P_{ref}) ds + \int_{s_y} \tau_{wx} ds \right]$$

Where τ_{wx} is the skin-friction component in the x-direction, s_x denotes the vertical surfaces of the block whose normal is in x-direction, and s_y denotes the floor and horizontal surfaces of the blocks whose normal is in y-direction. The friction factor and friction velocity are then defined as:

$$(12) f = \frac{8\tau_x}{\rho U^2} ; u_\tau = \sqrt{\tau_x / \rho}$$

Where \bar{U} is the average velocity obtained by integration of the velocity profile from the lower wall to the velocity maximum at $y = \delta$.

The numerical model was again used to simulate the flow in channels with different block arrangement, varying the block height and the Reynolds number.

Fig. 6 shows the space-averaged velocity profiles in wall coordinates for $c = 2b$ for three block heights and two Reynolds numbers. From these and similar plots for other geometries it is found that, in general, the velocity profiles have logarithmic regions for blocks in the in-line arrangement. The logarithmic regions are better defined as the block size is reduced and/or the Reynolds number is increased, as might be expected from the extent of the disturbance introduced by the blocks. With the staggered blocks, however, the flow is

disturbed so much that a well-defined logarithmic region exists only for sufficiently small block heights, typically less than 5% of the channel height. In other words, taller blocks cannot be regarded as roughness in the traditional sense, and consequently, it is not appropriate to use correlations for friction and heat transfer based on the logarithmic velocity profile. All profiles for rectangular blocks in in-line arrangement and for square blocks in either arrangement (not shown) contain a logarithmic region.

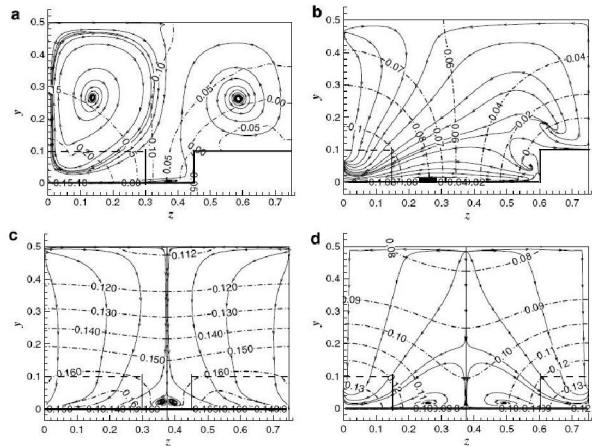


Figure.5. Cross-flow patterns and pressure (β) distributions at $x/D_s = 0.6$ for $w/h = 12, h/D_s = 0.1$, and $Re_{D_s} = 20,000$: (a) $c = 2b$ (staggered); (b) $c = b$ (staggered); (c) $c = 2b$ (in-line); (d) $c = b$ (in-line)

As in the case of two-dimensional ribs, the resistance coefficients and roughness functions for $h/D_s = 0.1$ are shown in Fig. 7 and 8, respectively.

Some values of ΔB for this block height are estimated, as the logarithmic region could not be clearly identified for some block arrangements. The results for two-dimensional ribs of the same relative height and length to height ratio are also shown for comparison. It is seen that the friction factor and the roughness function attain maximum values somewhere between $w/h = 10$ and 15, which is very similar to two-dimensional cases. The block spacing that results in maximum drag is often associated with the point of maximum heat transfer, which is the subject of Part II of this paper. It is interesting to observe that the resistance for blocks of square cross-section is comparatively small and identical for both block arrangements while that for the rectangular block is larger and there is substantial difference between the in-line and staggered arrangements. For the rectangular blocks, the in-line arrangement gives a smaller resistance, even smaller than the two-dimensional ribs, while the staggered arrangement exerts much larger resistance on the flow than the two-dimensional ribs. This is due to the fact that the fluid has to turn more wildly to go around the

staggered blocks and, hence creates a much greater disturbance in the outer flow when the block is tall. This was confirmed by additional calculations with smaller blocks. As in two-dimensional cases, the roughness

function ΔB varies logarithmically with slope $1/k$ with increasing h^+ .

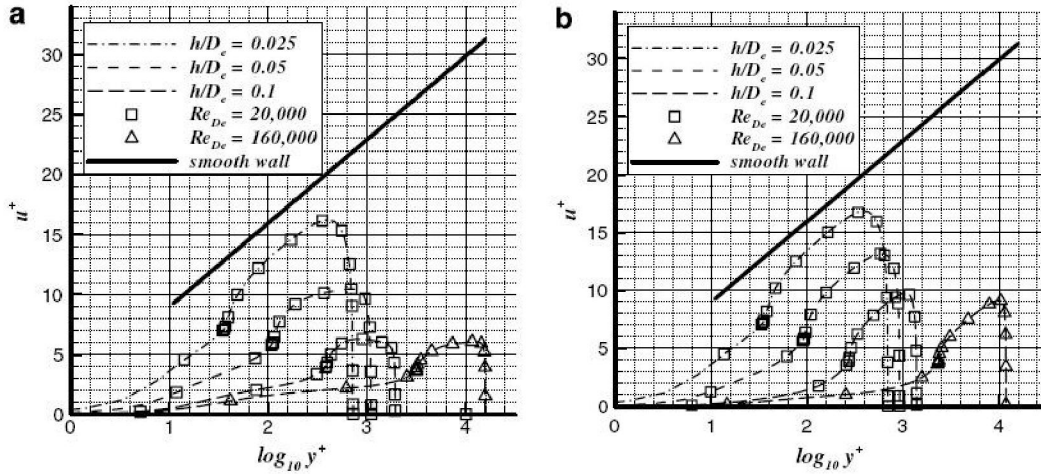


Figure.6. Mean stream wise velocity profiles in wall coordinates for $w/h = 12$ and $c = 2b$ with various block heights: (a) staggered arrangement; (b) in-line arrangement.

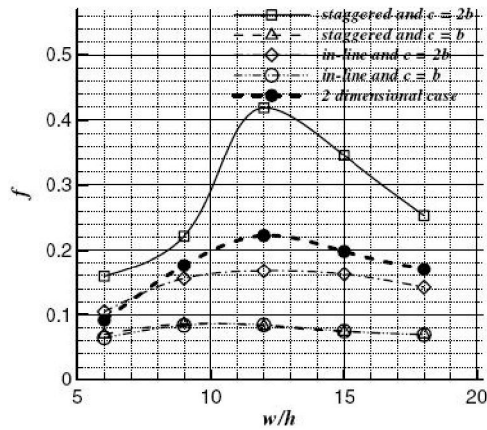


Figure.7. Friction factor vs. pitch for $h/D_c = 0.1$ at $Re_{D_c} = 20,000$.

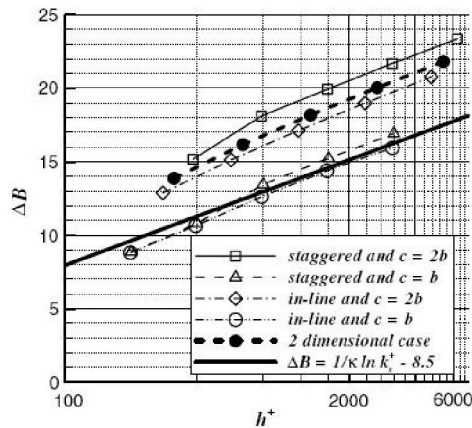


Figure.8. Roughness functions vs. pitch for $h/D_c = 0.1$ at $Re_{D_c} = 20,000$.

4. Conclusions

The most important conclusion drawn from this research is that a numerical model based on the Reynolds-averaged Navier-Stokes equations coupled with a turbulence model that resolves the near-wall flow is able to successfully capture the essential features of the flow over the three-dimensional blocks. When the solutions are averaged over appropriate areas, they provide engineering information about the resistance coefficient and its dependence on the geometric and flow parameters.

In addition, the numerical model provides details of the velocity profile, such as the roughness function and the virtual origin, that have hitherto for been the purview of experimental correlations, and information about the flow in the roughness layer, within the interstices of the roughness elements, that is difficult to measure and quantify by experiments. Although the latter aspects of the solutions have not been examined in any detail in the present paper, they are of interest in understanding the interaction between the spatially non-uniform flow in the roughness layer and the outer flow that feels only an averaged effect of a rough wall. Previous experience with contemporary turbulence models suggests that use of alternate models will confirm the principal results of this study.

For three-dimensional flows, the logarithmic region exists for blocks typically less than 5% of the channel height. Thus, the flow over larger blocks cannot be treated within the traditional framework of surface roughness that is based on the assumption of a logarithmic layer. Of course, this does not diminish the usefulness of the numerical model. On the contrary, a numerical model provides information that cannot be obtained by extrapolation of existing roughness correlations. The slope reaches the value of k^{-1} for sufficiently large h^+ , confirming the trends established by experiment for other types of roughness. For three-dimensional blocks, the resistance and the roughness function depend on the block shape and arrangement.

References

- [1] H.Schlichting, Boundary-Layer Theory, seventh ed. McGraw Hill, pp.598-634, 1979.
- [2] R.L.Webb, E.R.G.Eckert, R.J.Goldstein. Heat transfer and friction in tubes with repeated-rib roughness. Int. J. Heat Mass Transfer 14, 601-617, 1971.
- [3] E.M.Sparrow, W.Q.Tao. Enhanced heat transfer in a flat rectangular duct with streamwise-periodic disturbances at one principal wall. Trans. ASME J. Heat Trans. 105, 851-861, 1983.
- [4] Y. T. Chen, J. H. Nie, B. F. Armaly, H. T. Hsieh. Turbulent separated convection flow adjacent to backward-facing step-effects of step height. Int. J. Heat Mass Transfer 49, 3670-3680, 2006.

- [5] V.C.Patel, J.Y.Yoon, Application of turbulence models to separated flow over rough surfaces. ASME J. Fluids Eng. 117,234-241, 1995.
- [6] D.C.Wilcox, Turbulence Modeling for CFD, second ed. DCW industries, 1998.
- [7] T.Hayase, J.A.C. Humphrey, R.Grief. A consistently formulated QUICK scheme for fast and stable convergence using finite-volume iterative calculation procedure. J. Comput. Phys. 98,108-118, 1992.
- [8] J.C.Vogel, J.K.Eaton, Combined heat transfer and fluid dynamic measurements downstream of a backward facing step. Trans. ASME J. Heat transfer 107,922-929, 1985.
- [9] L.E.Drain, S.Martin. Two component velocity measurement of turbulent flow in a ribbed-wall flow channel In: International Conference on Laser Anemometry-Advances and Applications, Manchester, UK, 1985.
- [10] H.C.Chen, V.C.Patel, Near-wall turbulence models for complex flows including separation. AIAA J. 26, 641-648, 1988.
- [11] J. Nikuradse. Laws for flow in rough pipes. NACA TM, 1292, 1950.

11/1/2011